1 **Characterization Eclosion Hormone Receptor function reveals differential**
2 **hormonal control of ecdysis during *Drosophila* development.**
3

4 Valeria Silva[1,§], Robert Scott[2], Paulina Guajardo[1], Haojiang Luan[2], Ruben Herzog[3]
5 Benjamin H. White[2], and John Ewer[1,3]
6
7 [1]Instituto de Neurociencias, and Centro Interdisciplinario de Neurociencia de Valparaíso,
8 Universidad de Valparaíso, Valparaíso, Chile
9 [2]Laboratory of Molecular Biology, National Institute of Mental Health, NIH, Bethesda,
10 Maryland, USA
11 [3] Université de la Sorbonne, Institut du Cerveau - Paris Brain Institute - ICM, Inserm,
12 CNRS, Paris, France.
13 [§] Current address: Centre for Neural Circuits and Behaviour, The University of Oxford,
14 Oxford, UK
15
16 [3]Corresponding author.
17 Email: john.ewer@uv.cl
18 RUNNING TITLE: Eclosion Hormone function in *Drosophila* ecdysis
19 KEY WORDS: Neurohormone, guanylate cyclase, molting, neuromodulation,
20 neuropeptides, adult emergence, insects.
21

ABSTRACT

Neuromodulators and peptide hormones play important roles in regulating animal behavior. A well-studied example is ecdysis, which is used by insects to shed their exoskeleton at the end of each molt. Ecdysis is initiated by Ecdysis Triggering Hormone (ETH) and Eclosion Hormone (EH), which interact via positive feedback to coordinate the sequence of behavioral and physiological changes that cause exoskeleton shedding. Whereas the cell types targeted by ETH are well characterized, those targeted by EH have remained largely unknown due to limited characterization of the EH receptor (EHR). A gene encoding an EHR has been described in the oriental fruit fly, *B. dorsalis*, and in the desert locust, *Schistocerca gregaria*. However, little is known in these species about its expression pattern and its precise role at ecdysis, and no other insect EHRs are known. Here we analyze CG10738, the *Drosophila* ortholog of the *B. dorsalis* gene encoding EHR, and show that expressing it in cells confers sensitivity to EH. In addition, mutations of CG10738 specifically disrupt ecdysis, phenocopying the knockout of the EH gene. Together, these results indicate that CG10738 encodes the *Drosophila* EHR. As in *B. dorsalis*, EHR is expressed in the ETH-producing Inka cells; in addition, it is expressed in many known targets of ETH, including the neurons responsible for the secretion of other ecdysis-related peptides, such as CCAP and EH itself. Our results from targeted knockdown and rescue experiments reveal that EHR is required for ecdysis in diverse cell types and that the role of EHR in different targets differs with developmental stage. Our findings indicate extensive convergence of EH and ETH signaling and provide an exemplar of the complex mechanisms by which hormones control animal behavior.

AUTHOR SUMMARY

Hormones and neuromodulators are important regulators of animal behavior. In insects, one of the best studied behaviors influenced by hormones is ecdysis, which allows the animal to shed the remains of its exoskeleton at the end of each molt. Ecdysis is controlled by two key hormones: Ecdysis Triggering Hormone (ETH) and Eclosion Hormone (EH). Whereas most targets of ETH have been identified, those of EH have remained largely unknown due to the limited characterization of its receptor, EHR. Previous studies identified a gene encoding EHR in the oriental fruit fly, *Bactrocera dorsalis*, and in the desert locust, *Schistocerca gregaria,* but little is known about its expression pattern or its precise role. Here, we show that CG10738 encodes the *Drosophila* EHR. We found that EHR is expressed in ETH-producing Inka cells, in neurons that secrete other ecdysis-related peptides, in addition to other neuronal classes and non-neuronal cells. Targeted knockdown and rescue experiments revealed that EHR is essential for ecdysis in various cell types, and that its role can vary depending on the developmental stage. Our findings reveal that the role of EH at ecdysis is complex and provides insights into how hormones and neuromodulators regulate animal behavior.

INTRODUCTION

Peptide hormones and neuromodulators are one of the most diverse groups of signaling molecules found in animals [1]. These small chains of amino acids have diverse functions both within and outside the central nervous system (CNS) in regulating a wide range of processes that that include metabolism, stress responses, circadian rhythms, locomotion, sleep, feeding, learning, memory, and social interactions [2-10]. They also play a role in regulating developmental processes such as insect metamorphosis, growth, and

67 reproduction [11]. Through their multifaceted roles, peptide hormones and
68 neuromodulators have profound effects on the physiology and behavior of organisms,
69 highlighting their significance as essential modulators of neural communication [12, 13].
70 Determining the mechanisms by which peptides control behavior is challenging due to
71 the complexity of their actions. Indeed, they operate at different levels, involving various
72 signaling pathways and cellular processes. They can act rapidly or over prolonged
73 periods, and they may exert localized or widespread actions, affecting the entire CNS,
74 specific neurons, as well as targets outside the CNS [13-17]. The synergistic actions of
75 multiple peptides in interconnected networks further complicates efforts to understand
76 their complex roles in behavior and physiology.
77 Ecdysis provides a unique system in which to investigate the mechanism of peptide action
78 and the complex neuromodulation of a stereotyped behavior. This essential sequence of
79 behavioral and physiological events occurs in all arthropods, where it is used to shed the
80 remains of the old exoskeleton at the completion of each molt, and to then inflate, harden,
81 and pigment the exoskeleton of the next stage. This innate behavior includes three
82 distinct and highly stereotyped phases: pre-ecdysis, ecdysis, and post-ecdysis, each
83 characterized by specific timing and coordinated movements [18, 19]. Any disruption or
84 alteration in these ecdysis phases can have severe consequences including death.
85 Ecdysis is controlled by a complex interaction of neuropeptides and peptide hormones
86 acting in a sequential order on the CNS [18, 20, 21]. Our current understanding of the
87 endocrine bases of ecdysis proposes that ecdysis is initiated by the release of Ecdysis
88 Triggering Hormone (ETH) from epitracheal cells (Inka cells) and of Eclosion Hormone
89 (EH) from the ventromedial neurons (Vm) in the brain. These two peptides trigger each

90 other's release, establishing an endocrine positive feedback that causes the sudden and
91 near-complete release of both peptides [22-24] and provides an unambiguous, all-or-
92 nothing, endocrine signal that triggers ecdysis. ETH and EH then act within the CNS, and
93 previous work has provided information on the identity of many of the neurons that
94 express the ETH receptor (ETHR) as well as on their timing of activation [25, 26]. Thus,
95 ETH acts on neurons that express the neuropeptides, Crustacean Cardioactive Peptide
96 (CCAP), Myoinhibitory Peptide (MIPs), Bursicon, FMRF-amide (FMRFa), and Leucokinin,
97 as well as on a large number of other peptidergic and non-peptidergic targets [19, 26, 27].
98 Although it is known that the actions of EH are not limited to causing ETH release but that
99 it also acts within as well as outside of the CNS to control ecdysis [28, 29], the identity
100 and function of the EH targets are not known.
101 Here, we focus on the role of EH at ecdysis by identifying and characterizing the neurons
102 and cells that express the EH receptor (EHR) in *Drosophila*. First, we confirmed that EHR
103 is encoded by the CG10738 gene, the ortholog of a gene in *B. dorsalis* previously
104 identified as an EHR [30]. We then used the Trojan exon technique [31] to generate an
105 EHR-GAL4 driver and Split Gal4 hemidrivers, which we used to determine the expression
106 pattern of the receptor and the function of EH targets as well as their pattern of activation
107 during ecdysis. As expected, EHR is expressed in ETH-producing Inka cells. In addition
108 it is expressed in the Vm neurons, which produce the EH neurohormone, suggesting that
109 EH may participate together with ETH in an endocrine feedback mechanism that
110 regulates EH release. EHR is also expressed in CCAP neurons, as well as many other
111 neurons that express ETHR, revealing a convergence of the EH and ETH signaling
112 systems. We found that disabling EHR function, silencing, or killing all EHR-expressing

113 cells, was lethal at larval ecdysis, phenocopying the deficits of *Eh* null mutants [28]. By
114 contrast, in some cases silencing EHR expression in specific subsets of cells only
115 affected pupal or adult ecdysis, suggesting the existence of stage-specific EH targets or
116 of targets that are essential only to ecdysis to a particular stage. Finally, we found that
117 restoring EHR function in subgroups of EHR-expressing cells rescued normal ecdysis
118 only partially and in a stage-dependent manner, suggesting that normal ecdysis may
119 require EHR expression in diverse cell types, whose relevance may vary across different
120 molts. Our findings underscore the complexity of the neuroendocrine control of ecdysis
121 and enhance our understanding of the mechanisms by which neuropeptides function and
122 modulate animal behaviors.

123 **RESULTS**

124 **CG10738 gene function is required for EH-induced ETH release from Inka cells.**

125 Previous research in the Oriental fruit fly, *Bactrocera dorsalis*, provided strong evidence
126 that a gene homologous to the *Drosophila* CG10738 gene encodes an EH receptor
127 expressed in the Ecdysis Triggering Hormone (ETH)-producing epitracheal "Inka" cells
128 [30]. To determine whether this receptor guanylyl cyclase has EHR activity, we
129 determined whether genetic lesions in CG10738 (see Fig. S1) affected the ability of
130 synthetic EH to trigger the release of ETH from "Inka" cells *in vitro*, which are known EH
131 targets [22]. As shown in Fig. 1A and quantified in Fig. 1F (see also Table S3), we found
132 that trachea from control (w^{1118}) 1st instar larvae at the dVP stage (double Vertical Plate;
133 approximately 25 min prior ecdysis to the 2nd instar; [32]) challenged with 1 nM of synthetic
134 EH released ETH from epitracheal cells in amounts similar to the near complete depletion

135 of ETH that is seen in control animals at the end of ecdysis (Fig. 1C). By contrast, no such
136 release was observed (Fig. 1B) in trachea from larvae *trans*-heterozygous for a genetic
137 deletion, *Df(3L)Exel9017* (called here *Df(3)EHR*) which includes CG10738, and either a
138 *Minos* insertion within exon 4 of CG10738 (called here *Mi*{*EHR*}) or a Trojan GAL4 driver
139 in which GAL4 was inserted in the intron between exons 10 and 11, which was designed
140 to interrupt the CG10738 gene (called here EHR-GAL4)(Fig. S1). A similar result was
141 obtained in intact mutant animals examined 2h after dVP stage (Fig. 1D and quantified in
142 1G; see also Table S3).

143 **Mutations in EHR cause lethal phenotypes during ecdysis behavior.**

144 We next evaluated the behavior of animals *trans*-heterozygous for the *Minos* insertion in
145 CG10738 or the GAL4 insertion in CG10738, and *Df(3L)Exel9017*. As summarized in Fig.
146 2, these mutant animals expressed at ecdysis phenotypes similar to those observed in
147 *Eh* null animals [28]. Indeed, they spent at least four times longer performing ecdysis-like
148 behaviors compared to controls (w^{1118}); they also did not express the pre-ecdysial phase
149 of the behavior, and the majority failed to shed their old cuticle, often dying trapped within
150 the old exoskeleton, and expressing the “buttoned-up” phenotype (Fig. 2A, B; see also
151 Table S3) first described for ETH mutants [32]. Overall, approximately 80% of EHR
152 mutant larvae failed to survive the first ecdysis (Fig. 2E). Although most mutant larvae
153 (~70%; Fig. 2C) completely filled their trachea with air, they took approximately 25 min to
154 do so in contrast to approximately 1 minute for control animals (Fig. 2D). The ca. 20% of
155 animals of either EHR mutant genotype that succeeded in shedding their old cuticle
156 eventually all died during the 2nd to 3rd larval ecdysis or during the pupal ecdysis.
157 Importantly, both the behavioral and the tracheal defects of these mutant combinations

158 were substantially rescued by expressing CG10738 in the EHR-expressing cells using a
159 Trojan exon GAL4 driver inserted in gene CG10738 (Fig. 2; Table 2 and Table S3).
160 The lethal phenotype exhibited by CG10738 mutants during ecdysis (Fig. 2) and the
161 requirement of EHR function in ETH cells for the release of ETH upon stimulation with
162 synthetic EH (Fig. 1), provide direct evidence that CG10738 encodes the *Drosophila* EH
163 receptor (EHR). The similarity of the EHR mutant phenotypes to those exhibited by
164 animals lacking a functional EH gene further suggests that this is the only EH receptor in
165 *Drosophila.*

166 **CG10738-expressing cells are necessary for larval, pupal, and adult, ecdysis.**

167 To determine the role of cells expressing CG10738 during larval, pupal, and adult ecdysis
168 we first examined the consequences of inactivating or ablating all EHR-expressing cells
169 using the inwardly rectifying potassium channel, *Kir2.1* [33], or the apoptotic inductor,
170 *reaper* [34], respectively. In both cases we observed that virtually all larvae exhibited
171 severe ecdysis deficits, including an extended locomotory phase, an absent or atypical
172 pre-ecdysis phase, and an ecdysial phase that lasted at least 10 times longer than normal
173 and was ultimately unsuccessful (Fig. 3A, D; cf. Table S3), with larvae dying trapped
174 within their old cuticle with severe deficiencies in tracheal air filling (Fig. 3B-C). We also
175 used the TARGET system [35] to conditionally inactivate the CG10738-expressing cells
176 24h before pupal and adult ecdysis and found that this also caused a lethal phenotype
177 during the corresponding ecdysis (Fig. 3E, F). Similarly, activation all the EHR-expressing
178 cells using the temperature-sensitive cation channel, *TrpA1*, for two hours prior to pupal
179 or adult ecdysis caused 100% lethality (Fig. S2). These results demonstrate that
180 CG10738-expressing cells are essential for larval, pupal, and adult ecdysis. They also

181 suggest that the timing and the sequence of activation of EH targets is critical for the
182 proper orchestration of ecdysis.

183 **EHR is expressed in ETH-producing Inka cells, in tracheal cells, in the CNS, as well**
184 **as in other tissues, during all developmental stages.**

185 We used EHR-GAL4 to identify cellular targets of EH. Importantly, we found that EHR is
186 expressed in ETH-producing Inka cells (Fig. 4A-C), consistent with our previous results
187 showing that EH-induced ETH release from these cells requires EHR function (Fig. 1).
188 EHR is also expressed in tracheal cells (Fig. 4D-E), where it plays an essential role in the
189 rapid inflation of the new tracheal tubes that occurs at ecdysis (Figs. 2,3; [36, 37]). We
190 also observed that EHR is expressed throughout all developmental stages in some body
191 wall cells (Fig. S3C, E) and in the proboscis of the adult (Fig. S3E). Finally, we observed
192 EHR expression in leg imaginal discs (Fig. 4F), which are associated with Keilin's organ.
193 Interestingly, cells that ring Keilin's organ have been reported to express EH [29], which
194 suggests a developmental signaling between this sensory structure and the developing
195 leg.

196 We also found that EHR is broadly expressed in the larval (Fig. 5) and pharate adult (Fig.
197 6) CNS. In particular it is expressed in CCAP neurons at both stages (Figs. 5B, 6B), which
198 was also expected based on work from other insects [38]. By contrast, EHR expression
199 in EH-producing Vm neurons (Figs. 5C, 6C) was not expected, and suggests that the EH
200 neuropeptide may participate together with ETH in controlling EH release.

201 We then used Split Gal4 hemidrivers to further identify neurons that expressed EHR (for
202 these drivers, GAL4 activity is reconstituted only in cells that express both a GAL4 DNA
203 binding domain and a transcription activation domain, thereby making them intersectional

204 tools). Using this tool, we further confirmed EHR expression in neurons expressing CCAP
205 (Fig. 5D, 6D,D') and in Vm neurons (Fig. 5E; 6E, E'; arrows), both of which also express
206 the ETH receptor [26], as well as in the DI EH neurons of the adult (Fig. 6E; arrowheads).
207 We also found that EHR is expressed in neurons that express the ETH receptor (ETHR,
208 isoforms A and B) (Fig. 5I-K, 6I,I'-K,K'), thereby revealing a notable level of convergence
209 between the signaling of EH and ETH. In addition, we found that EHR is expressed in
210 neurons that express the CCAP receptor (CCAP-R) (Fig. 5F, 6F,F'), and the bursicon
211 receptor, *rickets* (*rk*) (Fig. 5H, 6GH,H'), which are receptors of peptide hormones that act
212 downstream of EH and ETH [17]. Bursicon itself is co-expressed in a subset of CCAP-
213 expressing neurons, which, as expected, express EHR (Fig. 5G, 6G,G'). These results
214 reveal that EH may control ecdysis through both feed forward and feedback mechanisms.
215 Finally, the use of split GAL4 drivers showed that EH targets also include glutamatergic
216 and cholinergic neurons (Fig. 5L-M, 6L,L'-M,M').

217 **Downregulating EHR in specific subsets of EHR-expressing cells causes lethal**
218 **phenotypes.**

219 In order to determine the function during ecdysis of EHR in specific subsets of EH targets,
220 we knocked-down EHR expression in different cell types. To do so we expressed EHR
221 RNAi under the control of different GAL4 drivers (Table 1) and evaluated the effects on
222 larval, pupal, and adult ecdysis. We found that knockdown of EHR with the broadly-
223 expressed *tubulin*-GAL4 driver caused significant lethality at larval stages (failure at
224 ecdysis from 1st to 2nd instar and 2nd to 3rd instar was 47% and 95%, respectively), with
225 the few (4) remaining 3rd instar larvae failing to ecdyse to the pupal stage. Overall, few of
226 the spatially more restricted GAL4 drivers tested caused significant ecdysial defects when

227 used to knockdown EHR expression (Table 1). Exceptions to this were GAL4 drivers
228 expressed in peptidergic neurons (*C929*-GAL4 which drives expression in *dimmed*-
229 positive peptidergic neurons; [39, 40] and secretory cells (*386Y*-GAL4; [41]), the ETH
230 cells and EH neurons, and tracheal cells (*btl*-GAL4), each of which yielded ecdysis deficits
231 $\geq$ 20% at least one stage. Interestingly, the impact of the knockdown was not uniform
232 across developmental stages, and differences occurred even between the seemingly
233 equivalent first and second larval ecdyses. Thus, for instance, knockdown of EHR in ETH
234 cells caused most animals (69%) to fail at the second to third instar larval ecdysis,
235 whereas no effect was observed at the first ecdysis. Similarly, knockdown of EHR in
236 trachea significantly affected pupal and adult ecdysis, but did not affect larval ecdysis.
237 Whether these results reveal stage-specific differences in the control of ecdysis or are
238 simply the result of varying knockdown efficiency is unknown. (Knockdown efficiency may
239 vary with driver strength, which itself may vary with developmental stage. Differences in
240 driver strength likely account for such effects as EHups-GAL4 causing more severe
241 phenotypes than the more widely expressed EHpan-GAL4 driver driver.) Interestingly,
242 knockdown of EHR using *n-syb*-GAL4 (neuron-specific driver) and *386Y*-GAL4 had no
243 effect on larval ecdysis but caused 100% failure at pupal ecdysis. This result suggests
244 that larval ecdysis may also require EH actions outside of the CNS. In this regard, it is
245 interesting to note that somatic sources of EH have previously been implicated in the
246 control of larval ecdysis [29]. Expression of EHR RNAi in CCAP neurons did not block
247 eclosion but caused wing expansion defects in over half of the animals, consistent with
248 the fact that CCAP is not essential for ecdysis in *Drosophila*, but is co-expressed with
249 bursicon, which controls wing inflation [42, 43]. Interestingly, although there is substantial

250 expression of EHR in ETHR positive neurons, we observed only modest defects in
251 animals bearing knockdown of EHR in ETH targets, suggesting that EH may reinforce the
252 response to ETH, but is not essential for ecdysial success. Finally, knockdown of EHR in
253 CCAP-R- and *rk*- expressing cells had no overt effect on ecdysis. Thus, although the
254 expression pattern of EHR suggests that EH may act on downstream elements of the
255 ecdysial cascade, any such feedforward action appears not to be essential for successful
256 ecdysis.
257 We were intrigued to observe EHR expression in body wall cells and in the proboscis
258 (Fig. S3C, E) because sensory neurons play a role at *Drosophila* pupation [44], and the
259 cibarial pump is activated at adult emergence in the moth, *Manduca sexta* [45].
260 Interestingly, EHR knockdown using GAL4 drivers expressed in several different
261 subgroups of sensory neurons (Ir25a, Ir7g, and 410-Gal4) impaired ecdysial success in
262 more than 10% of animals at least one developmental stage.

263 **Peptidergic neurons expressing EHR are sufficient to rescue ecdysis behavior in**
264 **EHR-mutants animals.**

265 In order to identify subsets of EHR-expressing cells that may play a critical role in the
266 control of ecdysis behavior, we investigated whether expression of EHR in particular
267 subsets of EH targets was sufficient to rescue the ecdysial failures caused by disabling
268 EHR function. For this, we determined whether expressing EHR using different GAL4
269 drivers could rescue the defects of animals mutant for EHR (mutant animals used were
270 *trans* heterozygous for *Df(3)EHR*, and either *Mi{EHR}* or *EHR*-GAL4). These results are
271 summarized in Table 2 and Fig. 8. As expected, expression of EHR using the EHR-GAL4
272 driver resulted in high levels of rescue (86-88% for larval ecdyses, and over 90% success

273 rate in subsequent ecdyses). By contrast, most other drivers tested produced limited
274 rescue. Overall, the most effective drivers were *C929*-GAL4 and *386Y-GAL4*, which are
275 expressed in peptidergic or secretory cells, respectively; of these, only *C929*-GAL4
276 rescued adult ecdysis, albeit only modestly. In addition, the results obtained were many
277 times stage-dependent and were greater for larval than for pupal or adult ecdyses, again
278 suggesting that some EH targets are preferentially involved in the control of some of the
279 fly's ecdyses. A caveat is that just as the absolute levels of knockdown are difficult to
280 evaluate due to the possible confounding effect of driver strength, the levels of rescue
281 obtained using different GAL4s are also difficult to compare quantitatively. For this reason
282 we identified drivers that produced "substantial rescue" based on whether they produced
283 levels of rescue that were greater than those seen in EHR mutant controls.

284 **EHR-expressing neurons show a complex pattern of activity during fictive pupal**
285 **ecdysis.**

286 In order to visualize the pattern of activity induced in EH targets at ecdysis, we used
287 synthetic ETH to stimulate the excised pupal CNS from animals expressing GCaMP6s
288 under the control of the EHR driver (as described in [25]). Figs. 7A-C and Supplementary
289 Video 1 shows the timecourse of activation of all individual EHR-expressing neurons after
290 hormonal stimulation *in vitro*. We observed that most neurons were active only during the
291 presumed ecdysial phase (min 10 to 30 of the recording), although a small group of
292 neurons became active earlier (which might correspond to the pattern of activity of fictive
293 pre-ecdysis) and others became active later, which might correspond to fictive post
294 ecdysis. Thus, as has been observed previously [19, 25], different targets of ecdysial
295 peptides respond at different times following the simultaneous stimulation with ETH,

296 revealing that a complex pattern of neuronal activity is set in motion following the sudden
297 release of the triggering neuropeptides, ETH and EH.

298 **Early Activation and Elevated Functional Coupling of CCAP Cells in the EHR**
299 **Population**

300 In order to understand the temporal dynamics within the EHR-expressing cell population,
301 we asked whether specific neuronal populations became active earlier and displayed
302 stronger functional coupling to the overall pattern of activity. To this end, we defined six
303 groups of neurons based on their position (Fig. 7B; Left and Right, which are likely made
304 up mostly of CCAP neurons; Central Left [CEN L], Central Right [CEN R], posterior
305 neurons [POS] and the remaining neurons ['REST']; see Methods for further details) and
306 computed their population coupling following Okun, *et al*. (2015) [46]. For this, we
307 calculated for each cell group and across 5 different videos, the cross-correlation function
308 between its activity and the average activity of the rest of the population (Fig. 7D). The
309 temporal position (Fig. 7E) indicated whether the cell became, on average, active before
310 or after the rest of the population and the maximum of this function served as an index of
311 population coupling strength (Fig. 7F).
312 Our analysis demonstrated that CCAP cells, and in particular the "Left" subgroup, reached
313 their peak coupling approximately 90 seconds prior to the activation of the rest of the
314 network ($p<0.05$, linear-mixed effect model with experiments as random effects). The
315 "Right" subgroup showed the same trend, but without significant effect ($p=0.17$).
316 Furthermore, the amplitude of the positive peak was significantly higher for both Left and
317 Right CCAP subpopulations compared to that of all other EHR-expressing populations
318 (Bonferroni corrected Wilcoxon rank sums $*p<0.05$).

319 These findings position CCAP cells as early activators within the EHR population,
320 exhibiting significantly higher functional coupling that may serve to prime subsequent
321 population-wide activity. The marked temporal precedence and enhanced coupling of
322 CCAP cells suggest that they play a critical role in orchestrating coordinated network
323 dynamics.

324 **DISCUSSION**

325 "Eclosion hormone" activity was described almost 50 years ago [47, 48], and EH has
326 since emerged as one of the main actors controlling ecdysis behavior in insects. However,
327 the breadth of its action has remained largely unknown because of the limited
328 characterization of its receptor. Here, we demonstrate that the gene CG10738 encodes
329 the *Drosophila* EH receptor (EHR) and show that it is expressed in all the cells and
330 neurons previously implicated in the control of ecdysis in addition to a large number of
331 neurons whose identity is mostly unknown. Interestingly, EH targets include the principal
332 EH-producing neurons, many ETH targets, as well as neurons that are targets of CCAP
333 and of bursicon, which act downstream of EH and ETH. This pattern of expression
334 suggests that EH and ETH control ecdysis via complex neuromodulatory feedback and
335 feedforward loops. The broad importance of EH signaling in the control of ecdysis is
336 underscored by the phase- and stage-specific effects of manipulations of EHR function in
337 subsets of EH targets. Thus, whereas some subsets were essential for the proper
338 execution of all ecdyses, others were required for only pupal and adult ecdysis.
339 Interestingly, we failed to find small subsets of EHR-expressing targets that were
340 sufficient to rescue the ecdysial defects of most individuals of a given genotype,
341 suggesting that many of the EH targets are important for successful ecdysis.

342 Nevertheless, our findings underscore the relevance for successful ecdysis of EHR
343 expression in ETH cells, in trachea, and in *dimmed*-expressing peptidergic neurons
344 (which are defined by the C929 GAL4 driver; [39, 40]).
345 Although the majority of neuropeptide receptors belong to the G protein-coupled
346 receptors (GPCRs) family [49], the EH receptor belongs to the family of guanylyl cyclase
347 receptors (GCR). Previous research by Chang *et al.*, (2009)[30] characterized the GCR,
348 BdmGC-1, from the Oriental fruit fly, *Bactrocera dorsalis*, and showed that it mediates
349 robust increases of cGMP following exposure to EH, when expressed in HEK cells. They
350 also showed that BdmGC-1 is strongly expressed in the epitracheal ETH cells and that
351 these cells respond with an increase in cGMP-immunoreactivity to an in vitro challenge
352 with synthetic EH. Recently, Verbakel *et al.* (2024) [50] showed that knockdown of the
353 locust ortholog of BdmGC-1 causes failures at ecdysis. Our results here confirm that the
354 *Drosophila* ortholog of BdmGC-1, CG10738, encodes the *Drosophila* EH receptor and
355 greatly extend what is known about EHR distribution and function.
356 Although EH is known to act within the *Drosophila* CNS [28], neuronal targets of EH have
357 not been identified directly. In many insects, cGMP-immunoreactivity (cGMP-IR)
358 increases at ecdysis in CCAP neurons [51, 52] This is also true in some dipterans, such
359 as mosquitoes, but has not been observed in *Drosophila*, where increases in cGMP-IR
360 have been detected in ETH producing Inka cells [36], but not CCAP neurons [52].
361 Furthermore, CCAP neurons (and CCAP itself) are not required for larval ecdysis in
362 *Drosophila* [53], suggesting that other neurons (in addition to or instead of) CCAP neurons
363 must express an EH receptor. Here we show that EHR is widely expressed in hundreds
364 of neurons including CCAP neurons, as well as in the trachea and epitracheal cells. Why

365 all these targets do not show increases in cGMP at ecdysis remains unknown, but may
366 be due to the sensitivity of the anti-cGMP antibody [52].
367 Interestingly we found significant colocalization of EHR and ETHR within the CNS,
368 revealing that EH and ETH not only coordinate each other's release, but share common
369 targets in the control of ecdysis. In addition, EHR is expressed in the principal EH-
370 producing Vm neurons themselves and is also co-expressed with receptors to
371 neuropeptides that have historically been viewed as acting downstream of EH (such as
372 bursicon and CCAP*)*. Thus, these results indicate the presence of both feedback and
373 feedforward loops in EH signaling. Coherent feedforward loops in which both signals
374 coordinately activate a downstream target are often used to filter transient activation by a
375 primary signal and delay the onset of full activation [54]. Such features might underlie, at
376 least in part, the sequential release of neuropeptides during ecdysis and the serial
377 activation of the different ecdysis phases. In addition, we find considerable convergence
378 of EH and ETH signaling, including at the Vm and CCAP/bursicon neurons. This
379 convergence suggests synergistic physiological effects of the two signaling systems on
380 downstream neurons, perhaps to dynamically regulate excitability, though this remains to
381 be determined. In any case, the architecture of control revealed here, with EH and ETH
382 mutually reinforcing each other's release and coordinating each other's downstream
383 actions, is reminiscent of the architecture of developmental gene regulatory networks, in
384 which transcriptional determinants establish a regulatory state and then activate
385 downstream inductive signals [55].
386 In addition to the CNS, we found that EHR was expressed in the epithelial cells of the
387 trachea, including cells from the primary tubular branch, secondary branches, and

388 terminal branches (Fig. 4C, D), and that knockdown of EHR in trachea caused failures at
389 ecdysis. These findings are consistent with previous reports that showed that ablating the
390 Vm neurons [37] or disabling the *Eh* gene [28] caused defects in the vital process of
391 tracheal air-filling that occurs during ecdysis. These defects cannot be rescued by
392 injections of ETH [36] indicating that they are due to the action of EH and are not due to
393 the absence of ETH release associated with these genotypes.
394 Although the identity of all EH targets largely remains to be determined, the relatively
395 penetrant effects of EHR suppression in sets of peptidergic neurons, as opposed to
396 neurons that use fast neurotransmitters (see Table 1), suggests that EH signaling is most
397 important in modulating cells in the ecdysis network above the level of the synaptic
398 networks that directly generate behavior. This is consistent with a model in which
399 modulatory interactions regulate behavioral state, which is then translated into the
400 execution of state-specific motor programs. The fact that both ecdysis motor programs
401 and the function of subsets of EHR-expressing cells vary with developmental stage
402 suggests that either the identity or the importance of the downstream factors recruited by
403 EH changes over development. This plasticity in ecdysis peptide usage is also seen
404 phylogenetically, with the complement of essential ecdysial peptides varying across
405 insect species. For example, whereas CCAP and orkokinin are dispensable for ecdysis
406 in *Drosophila* [53, 56], both are essential in the kissing bug, *Rhodnius prolixis* [57, 58].
407 The stage-dependent differences in function of both ecdysial peptides and the cell types
408 that express them in *Drosophila* may, in fact, simply reflect necessary differences in the
409 control and generation of the ecdysis motor programs that evolved to accommodate
410 metamorphosis and its attendant changes in body plan [59]. Overall, our results suggest

411 an intricate interplay between multiple cell types and between multiple neuromodulatory
412 peptides in regulating ecdysis. Understanding of how this complex behavior is controlled
413 in *Drosophila* and, potentially, in other species, should contribute to our understanding of
414 how neuromodulation mediated by neuropeptides regulates animal behaviors.

415
416

417 **MATERIALS AND METHODS**

418 **Fly strains**

419 Fly stocks were maintained at room temperature (22-25ºC) on standard cornmeal agar
420 media under a 12 h light/12h dark regime. Stocks used and their source are listed in Table
421 S1.

422 **EHR-GAL4 generation**

423 The EHR-GAL4 line was made by inserting a Trojan Gal4 Expression Module (TGEM)
424 [31] into the intron separating exons 10 and 11 of the CG10738 gene (Fig. S1). Insertion
425 was targeted to the following site using CRISPR/Cas9:
426 AAATGTGGGCTGTACTTATTAGG (PAM site underlined). To make the TGEM
427 construct, homologous arms of 1 kb flanking the Cas9 cleavage site were amplified by
428 PCR using the following primer pairs synthesized by Integrated DNA Technologies, Inc.
429 (Coralville, Iowa, USA):
430 EHR-3NotI: AGTCAG GCGGCCGC AAGTACAGCCCACATTTTGC,
431 EHR-3AgeI: AGTCAG ACCGGT TGATGGAAGTCCTGGATTCG,
432 EHR-5SpeI: AGTCAG ACTAGT AATAGGCATCCCCTCGTTGT,
433 EHR-5AscI: AGTCAG GGCGCGCC ATTAGGTTATTTTAAAGTGCATGCAGAAGG,
434 The PCR products were cloned into the pT-GEM(0) vector. The resulting plasmid (250-
435 pGS3-AgeI-NotI-arm-SA-T2AGal4-hsp70-3xP3-RFP-SV40-AscI-EHRarm) was co-
436 injected with a pBS-U6-sgRNA-ETH plasmid encoding the guide RNA into embryos of
437 flies expressing germline Cas9 as described previously [31]. Transformants were
438 identified by their expression of the 3xP3-RFP marker. The EHR Split-GAL4 hemidriver

439 lines were generated from the EHR-Gal4 strain by ΦC31-mediated cassette exchange as
440 described in Diao *et al.,* (2015) [31].

441 **UAS-EHR generation**

442 GC10738 cDNA was amplified from *Drosophila* larval CNSs using standard methods. The
443 entire coding sequence was re-amplified using primers that included XhoI and KpnI sites
444 at the 5' and 3' ends, respectively. Correct sequence was confirmed and the XhoI-KpnI
445 fragment (containing the entire CG10738 coding sequence) was cloned into pUAST
446 transformation vector by Genewiz (New Jersey, USA). Transformants were generated by
447 BestGene (California, USA).

448 **EH synthesis**

449 Synthetic EH was produced by GenScript (Hong Kong) using the pFastBac baculovirus
450 expression system. Several constructs were tested with the goal of producing a secreted
451 protein with high yield. Best results were obtained with a design that included the putative
452 native signal sequence (vs. the signal sequence of the major envelope glycoprotein,
453 gp67) and a His-tag at the amino-terminal of the protein. The sequence of the expressed
454 protein was (putative mature EH sequence underlined):
455 MNCKPLILCTFVAVAMCLVHFGNAHHHHHHENLYFQG<u>LPAISHYTHKRFDSMGGIDFV</u>
456 <u>QVCLNNCVQCKTMLGDYFQGQTCALSCLKFK GKAIPDCEDIASIAPFLNALE</u>
457 Analysis indicated that the protein was not secreted and it was therefore purified from the
458 cell lysate. It was then aliquoted in 50 mM Tris-HCl, 500 mM NaCl, 5% Glycerol, pH 8.0
459 at a concentration of 0.25 mg/ml and stored at -20°C.

460 **Stimulation with synthetic EH**

461 Larvae were reared at 25ºC on Petri dishes with fly medium. First instar larvae
462 approaching ecdysis to the second instar were identified by their double mouth hooks
463 (dMH), placed on Petri dishes coated with apple juice agar, and monitored until they first
464 pigmented the plates of the second instar (double vertical plate stage, dVP, approximately
465 25 min prior ecdysis to the 2nd instar; [32]. Their tracheae were then dissected in PBS and
466 incubated in Schneider's insect medium (Sigma). All tracheae of the same genotype
467 dissected within 20 min were pooled; then were challenged either with synthetic EH (1nM
468 final concentration) or the same volume of water. After 1h incubation at room temperature
469 the tracheae were fixed and processed for ETH immunoreactivity [32], as described
470 below. Tracheae from wild type animals prior to ecdysis as well as from larvae post-
471 ecdysis were included as controls. In the case of animals mutant for EHR (which do not
472 ecdyse) tracheae were dissected 2h after the dVP stage.
473 All epitracheal cells were imaged using the same parameters using an Olympus DSU
474 spinning disk microscope (40x oil objective Olympus). The intensity of ETH
475 immunoreactivity (ETH-IR) of each epitracheal cell was scored blind and assigned a score
476 from 0 (no detectable ETH-IR) to 3 (maximal ETH-IR). Thirty to 60 cells were measured
477 per conditions, representing the tracheae of 3-7 animals.

478 **Immunohistochemistry**

479 Preparations were dissected on Sylgard-coated plates under cold PBS and fixed in 4%
480 paraformaldehyde for 1h at room temperature or overnight at 4ºC, as previously described
481 in Clark, *et al.* (2004) [36]. Tissues were then rinsed several times in PBS with 0.3% Triton
482 X-100 (Sigma) (PBSTX) and incubated in primary antibodies overnight at 4°C with

483 constant agitation. Then they were washed in PBSTX and incubated in fluorescent
484 secondary antibodies (Jackson ImmunoResearch, West Grove, PA) and mounted onto
485 poly-L-lysine (Sigma) coated coverslips. Primary antibodies used include: rabbit anti-
486 CCAP ([52]; used at 1:500), rabbit anti-ETH ([32] used at 1:2,000) and rabbit anti-EH
487 ([28]; used at 1:200). For GAL4 lines that produced low GFP signal when driving UAS-
488 GFP, tissues were processed using anti-GFP (Invitrogen; used at 1:1,000). Preparations
489 were viewed and imaged under a conventional fluorescent microscope or under an
490 Olympus DSU spinning disk microscope and analyzed using ImageJ [60].

491 **Survival across the different ecdyses**

492 To quantify the number of animals that successfully completed larval ecdysis, we placed
493 first instar larvae of the relevant genotype on Petri dishes with regular food and counted
494 the number of larvae that ecdysed to the second instar. These larvae were transferred to
495 Petri dishes with new regular food, and we then counted the number of animals that
496 ecdysed to the third larval instar. We then transferred these larvae to vials with regular
497 food, where we followed the success of pupal and adult ecdysis. For some genotypes we
498 preferentially focused on specific ecdyses.

499 **Quantification of larval ecdysis behavior**

500 Larvae were reared at 25ºC on Petri dishes with fly medium. First instar larvae at the dMH
501 stage were placed on Petri dishes coated with apple juice agar with yeast. At dVP larvae
502 were transferred individually to a new slightly wet agar Petri dish and video-recorded
503 under a Leica dissecting microscope (Nussloch, Germany) until they completed ecdysis
504 or for up to 2h after the time of ecdysis of control animals. Behavioral analysis scored for

505 the presence or absence of three different phases: “locomotion,” consisting of normal
506 locomotor activity; “pre-ecdysis,” consisting of anterior-posterior contractions (AP) and
507 squeezing waves (SW); and “ecdysis” which started with “biting” behavior and ended with
508 the final backward thrust, regardless of whether the old cuticle was eventually shed.
509 “Atypical pre-ecdysis” was defined by partial, weak, or missing AP contractions or SW (as
510 described previously in Scott, *et al*. (2020) [29]. Quantification of tracheal dynamics
511 included: (1) the time taken to completely fill the trachea with air; for those animals that
512 successfully completed that process and, (2) the percentage of animals that completed
513 the air filling process (if ≥ 95% of the trachea filled with air it was considered filled) or
514 failed.

515 **Quantification of pupal ecdysis and adult eclosion**

516 Flies were reared at 25ºC on standard cornmeal agar media under a 12 h light/12h dark
517 regime. Pupal and adult ecdysis survival and failure were evaluated as described in Lahr,
518 *et al*. (2012) [53]. For experiments using the TARGET system (temperature sensitive
519 GAL80^{ts}; [35]) or the temperature-sensitive cation channel, *TrpA1* [61], flies were reared
520 at 18ºC and transferred to 30ºC before pupal ecdysis or adult eclosion (24h hours before
521 ecdysis for GAL80^{ts}, and 2h for *TrpA1* flies), and ecdysis success or failure was
522 evaluated.

523 **RNAi screening**

524 Six different UAS-RNAi lines for CG10738 (see Table S2) were crossed with the *tubulin*-
525 GAL4 line and the severity of the ecdysial defects determined by counting the number of
526 larvae or pupae showing failures at ecdysis and the number of adults that emerged (see

527 Table S2). This screen revealed that line CG10738 RNAi-R1 produced the most severe
528 phenotype and is the one used here; it was always used in combination with UAS-*dicer2*
529 (UAS-*dcr2*) to boost the effectiveness of RNAi knockdown.

530 **Real-time GCaMP Imaging**

531 In order to record calcium dynamics in *in vitro* CNS preparations, CNSs were dissected
532 from animals around 2 hours prior to pupal ecdysis under cold 1X PBS and immediately
533 mounted on a poly-L-lysine coated glass, placed in an Attofluor chamber (Thermo-Fisher
534 Scientific), and covered with 2 mL of Schneider's insect medium (Sigma). GCaMP6s [62]
535 signal was recorded using an Olympus DSU spinning disk microscope with a 20X water
536 objective and a Hamamatsu high sensitivity camera. Preparations were first imaged for 5
537 min at 0.2 Hz, and preparations showing spontaneous activity were discarded. Synthetic
538 ETH (600 nM final concentration) or H_2O (control) was added and 5 Z-stacks across the
539 whole VNC were recorded for one hour at 0.2 Hz, as previously described in Mena, *et al*.
540 (2016) [25].

541 **Video analysis**

542 Real-time calcium imaging videos were processed using FIJI software (Schindelin et al.,
543 2012) to create hyperstacks and a maximum intensity projection (template). We then used
544 the FluoroSNNAP MATLAB program to select all ROIs that corresponded to the center of
545 each neuronal cell body and followed each of their activity during the 60 min recording
546 period to create at the time series of fluorescence intensity (Patel et al., 2015).
547 Calcium traces were normalized by using the previous 50 frames corresponding to 250 s
548 as baseline, obtaining the dF/F traces (as described in [63] and [64]).

549 **Manual selection of cell types**

550 We analyzed 5 different videos (n= 65.4 ± 10.78 cells; mean ± standard deviation), where
551 we defined six EHR cell populations: posterior cells (POS, n= 10.2 ± 2.2), Left neurons
552 (Left, n= 7.8 ± 0.40), Right neurons (Right, n= 6.8 ± 1.3), central cells Left (CEN L, n=
553 10.4 ± 2.4), central cells Right (CEN R, n= 10.2 ± 2.2) and the rest ("REST", n= 20.20 ±
554 13). These groups were defined by identity and their position within the VNC considering
555 a midline that symmetrically separate left and right side of the CNS.

556 **Population coupling function**

557 The functional population coupling function (PCF) of each cell was computed following
558 Okun, *et al*. (2015) [46]. We computed the lagged-cross correlation function between
559 each time series of one cell versus that of a 'population' time series, which was obtained
560 by averaging the activity of all the remaining cells of the population. To then characterize
561 the level and temporality of the coupling of each cell, the maximum of the function and its
562 location in terms of temporal lags were extracted. Using this measure, a positive lag
563 indicates that the population follows a given neuron, whereas a negative lag indicates
564 that the neuron follows the population activity.
565 A linear-mixed effect model with experiments as random effects was used to evaluate if
566 the lags associated with the maximum of the PCF were significantly different from zero.
567 One model was used for each cell type. Means were estimated from these models, using
568 the "REST" group as baseline. A Wilcoxon rank sums test was used to perform pairwise
569 comparisons between the maximum value of the PCF, and the p-values were corrected
570 by the Bonferroni method (15 comparisons).

571 **Statistics**

572 Statistical analyses were performed using GraphPad Prism (GraphPad Software, La
573 Jolla, CA, USA) and visualized using Adobe Illustrator. If data were normally distributed
574 and had equal variance, they were analyzed by one-way ANOVA followed by the Tukey
575 test for *post hoc* multiple comparison analyses. Categorical data were analyzed by Chi-
576 square or Fisher's exact test. The exact values for each comparison are shown in
577 Supplementary Table S3.

578 **ACKNOWLEDGMENTS**

579 We thank Eileen Krüger for amplifying CG10738 cDNA. We thank Vivian Budnik, Susan
580 McNabb, Paul Taghert, Rob Jackson, Christian Wegener, and the Bloomington, Kyoto
581 and Vienna, *Drosophila* stock centers for fly stocks, and Michael Adams for anti-ETH
582 antisera. This work was supported by CONICYT Graduate Fellowship 21191720 (to V.S.);
583 FONDECYT (National Fund for Scientific and Technological Development, Chile) grant
584 1221270 (to J.E.) and the Intramural Research Program of the National Institute of Mental
585 Health, USA (ZIAMH002800, to B.H.W.).

586 **REFERENCES**

587 1. Jékely G, Melzer S, Beets I, Kadow ICG, Koene J, Haddad S, et al. The long and the
588 short of it - a perspective on peptidergic regulation of circuits and behaviour. J Exp Biol.
589 2018;221(Pt 3). doi: 10.1242/jeb.166710.
590 2. Nassel DR, Zandawala M. Recent advances in neuropeptide signaling in *Drosophila*,
591 from genes to physiology and behavior. Prog Neurobiol. 2019;179:101607. doi:
592 10.1016/j.pneurobio.2019.02.003.

593 3. Schoofs L, De Loof A, Van Hiel MB. Neuropeptides as Regulators of Behavior in
594 Insects. Annu Rev Entomol. 2017;62:35-52.
595 4. Bhat US, Shahi N, Surendran S, Babu K. Neuropeptides and Behaviors: How Small
596 Peptides Regulate Nervous System Function and Behavioral Outputs. Front Mol
597 Neurosci. 2021;14:786471. doi: 10.3389/fnmol.2021.786471.
598 5. Feany MB. Neuropeptide modulation of learning and memory processes. Rev
599 Neurosci. 1996;7(2):151-64. doi: 10.1515/revneuro.1996.7.2.151.
600 6. Lee MC, Schiffman SS, Pappas TN. Role of neuropeptides in the regulation of feeding
601 behavior: a review of cholecystokinin, bombesin, neuropeptide Y, and galanin.
602 Neurosci Biobehav Rev. 1994;18(3):313-23. doi: 10.1016/0149-7634(94)90045-0.
603 7. Rigney N, de Vries GJ, Petrulis A, Young LJ. Oxytocin, Vasopressin, and Social
604 Behavior: From Neural Circuits to Clinical Opportunities. Endocrinology. 2022;163(9).
605 doi: 10.1210/endocr/bqac111.
606 8. Rigney N, de Vries GJ, Petrulis A. Modulation of social behavior by distinct vasopressin
607 sources. Front Endocrinol (Lausanne). 2023;14:1127792. doi:
608 10.3389/fendo.2023.1127792.
609 9. Shen YC, Sun X, Li L, Zhang HY, Huang ZL, Wang YQ. Roles of Neuropeptides in
610 Sleep-Wake Regulation. Int J Mol Sci. 2022;23(9). doi: 10.3390/ijms23094599.
611 10. Van Damme S, De Fruyt N, Watteyne J, Kenis S, Peymen K, Schoofs L, et al.
612 Neuromodulatory pathways in learning and memory: Lessons from invertebrates.
613 Journal of neuroendocrinology. 2021;33(1):e12911. doi: 10.1111/jne.12911.
614 11. Altstein M, Nassel DR. Neuropeptide signaling in insects. Adv Exp Med Biol.
615 2010;692:155-65. doi: 10.1007/978-1-4419-6902-6_8.

616 12. Iversen L. Neuropeptides: Regulators of Physiological Processes. Trends in
617 Neurosciences. 1999;22(10):482. doi: 10.1016/S0166-2236(99)01429-0.
618 13. Marder E. Neuromodulation of neuronal circuits: back to the future. Neuron.
619 2012;76(1):1-11. doi: 0.1016/j.neuron.2012.09.010.
620 14. Taghert PH, Nitabach MN. Peptide neuromodulation in invertebrate model systems.
621 Neuron. 2012;76(1):82-97. doi: 10.1016/j.neuron.2012.08.035.
622 15. van den Pol AN. Neuropeptide transmission in brain circuits. Neuron. 2012;76(1):98-
623 115. doi: 10.1016/j.neuron.2012.09.014.
624 16. Nadim F, Bucher D. Neuromodulation of neurons and synapses. Curr Opin Neurobiol.
625 2014;29:48-56. doi: 10.1016/j.conb.2014.05.003.
626 17. Diao F, Elliott AD, Diao F, Shah S, White BH. Neuromodulatory connectivity defines
627 the structure of a behavioral neural network. Elife. 2017;6:e29797. doi:
628 10.7554/eLife.29797.
629 18. Ewer J, Reynolds S. Neuropeptide control of molting in insects. In: Pfaff DW, Arnold
630 AP, Fahrbach SE, Etgen AM, Rubin RT, editors. Hormones, brain and behavior. 35.
631 San Diego, CA: Academic Press; 2002. p. 1-92.
632 19. Kim YJ, Zitnan D, Galizia CG, Cho KH, Adams ME. A command chemical triggers an
633 innate behavior by sequential activation of multiple peptidergic ensembles. Curr Biol.
634 2006;16(14):1395-407.
635 20. Zitnan D, Adams ME. Neuroendocrine regulation of ecdysis. In: Gilbert LI, editor.
636 Insect Endocrinology: Elsevier; 2012. p. 253-309.
637 21. White BH, Ewer J. Neural and hormonal control of postecdysial behaviors in insects.
638 Annu Rev Entomol. 2014;59:363-81.(doi):10.1146/annurev-ento-011613-162028.

639 22. Ewer J, Gammie SC, Truman JW. Control of insect ecdysis by a positive-feedback
640 endocrine system: roles of eclosion hormone and ecdysis triggering hormone. J Exp
641 Biol. 1997;200:869-81.
642 23. Kingan TG, Gray W, Zitnan D, Adams ME. Regulation of ecdysis-triggering hormone
643 release by eclosion hormone. J Exp Biol. 1997;200:3245-56.
644 24. Zitnan D, Kingan TG, Hermesman JL, Adams ME. Identification of ecdysis-triggering
645 hormone from epitracheal endocrine system. Science. 1996;271:88-91.
646 25. Mena W, Diegelmann S, Wegener C, Ewer J. Stereotyped responses of *Drosophila*
647 peptidergic neuronal ensemble depend on downstream neuromodulators. Elife.
648 2016;5.(pii):10.7554/eLife.19686.
649 26. Diao F, Mena W, Shi J, Park D, Diao F, Taghert P, et al. The Splice Isoforms of the
650 *Drosophila Ecdysis Triggering Hormone Receptor* Have Developmentally Distinct
651 Roles. Genetics. 2016;202(1):175-89. doi: 10.1534/genetics.115.182121.
652 27. Daubnerová I, Roller L, Satake H, Zhang C, Kim YJ, Žitňan D. Identification and
653 function of ETH receptor networks in the silkworm *Bombyx mori*. Sci Rep.
654 2021;11(1):11693. doi: 10.1038/s41598-021-91022-8.
655 28. Kruger E, Mena W, Lahr EC, Johnson EC, Ewer J. Genetic analysis of Eclosion
656 hormone action during *Drosophila* larval ecdysis. Development. 2015;142(24):4279-
657 87. doi: 10.1242/dev.126995.
658 29. Scott RL, Diao F, Silva V, Park S, Luan H, Ewer J, et al. Non-canonical Eclosion
659 Hormone-Expressing Cells Regulate *Drosophila* Ecdysis. iScience.
660 2020;23(5):101108. doi: 10.1016/j.isci.2020.101108.

661 30. Chang JC, Yang RB, Adams ME, Lu KH. Receptor guanylyl cyclases in Inka cells
662 targeted by eclosion hormone. Proc Natl Acad Sci U S A. 2009;106(32):13371-6.
663 31. Diao F, Ironfield H, Luan H, Diao F, Shropshire WC, Ewer J, et al. Plug-and-Play
664 Genetic Access to *Drosophila* Cell Types using Exchangeable Exon Cassettes. Cell
665 Rep. 2015;10(8):1410-21. doi: 10.016/j.celrep.2015.01.059.
666 32. Park Y, Filippov V, Gill SS, Adams ME. Deletion of the ecdysis-triggering hormone
667 gene leads to a lethal ecdysis deficiency. Development. 2002;129:493-503.
668 33. Baines RA, Uhler JP, Thompson A, Sweeney ST, Bate M. Altered electrical properties
669 in *Drosophila* neurons developing without synaptic transmission. J Neurosci.
670 2001;21(5):1523-31.
671 34. White K, Tahaoglu E, Steller H. Cell killing by the *Drosophila* gene *reaper*. Science.
672 1996;271:805-7.
673 35. McGuire SE, Mao Z, Davis RL. Spatiotemporal gene expression targeting with the
674 TARGET and gene-switch systems in *Drosophila*. Sci STKE. 2004;2004(220):pl6. doi:
675 10.1126/stke.2202004pl6.
676 36. Clark AC, Del Campo M, Ewer J. Neuroendocrine control of larval ecdysis behavior
677 in *Drosophila*: complex regulation by partially redundant neuropeptides. J
678 Neuroscience. 2004;24:4283-92.
679 37. McNabb SL, Baker JD, Agapite J, Steller H, Riddiford LM, Truman JW. Disruption of
680 behavioral sequence by targeted death of peptidergic neurons in *Drosophila*. Neuron.
681 1997;19:813-23.

682 38. Ewer J, Truman JW. Invariant association of ecdysis with increases in cyclic 3',5'-
683 guanosine monophosphate (cGMP)-immunoreactivity in a small network of peptidergic
684 neurons in the hornworm, *Manduca sexta*. J Comp Physiol. 1997;181:319-30.
685 39. Hewes RS, Park D, Gauthier SA, Schaefer AM, Taghert PH. The bHLH protein
686 *Dimmed* controls neuroendocrine cell differentiation in *Drosophila*. Development.
687 2003;130(9):1771-81.
688 40. Park D, Taghert PH. Peptidergic neurosecretory cells in insects: organization and
689 control by the bHLH protein DIMMED. General and comparative endocrinology.
690 2009;162(1):2-7.
691 41. Taghert PH, Hewes RS, Park JH, O'Brien MA, Han M, Peck ME. Multiple amidated
692 neuropeptides are required for normal circadian locomotor rhythms in *Drosophila*. J
693 Neurosci. 2001;21(17):6673-86.
694 42. Peabody NC, Diao F, Luan H, Wang H, Dewey EM, Honegger HW, et al. Bursicon
695 functions within the *Drosophila* CNS to modulate wing expansion behavior, hormone
696 secretion, and cell death. J Neurosci. 2008;28(53):14379-91.
697 43. Peabody NC, Pohl JB, Diao F, Vreede AP, Sandstrom DJ, Wang H, et al.
698 Characterization of the decision network for wing expansion in *Drosophila* using
699 targeted expression of the TRPM8 channel. J Neurosci. 2009;29(11):3343-53.
700 44. Elliott AD, Berndt A, Houpert M, Roy S, Scott RL, Chow CC, et al. Pupal behavior
701 emerges from unstructured muscle activity in response to neuromodulation in
702 *Drosophila*. Elife. 2021;10. doi: 10.7554/eLife.68656.
703 45. Miles CI, Booker R. The role of the frontal ganglion in the feeding and eclosion
704 behavior of the moth, *Manduca sexta*. J Exp Biol. 1998;201:1785-98.

705 46. Okun M, Steinmetz N, Cossell L, Iacaruso MF, Ko H, Bartho P, et al. Diverse coupling
706 of neurons to populations in sensory cortex. Nature. 2015;521(7553):511-5. doi:
707 10.1038/nature14273.
708 47. Truman JW, Riddiford LM. Neuroendocrine control of ecdysis in silkmoths. Science.
709 1970;167:1624-6.
710 48. Truman JW, Taghert PH, Copenhaver PF, Tublitz NJ, Schwartz LM. Eclosion
711 hormone may control all ecdyses in insects. Nature. 1981;291(5810):70-1.
712 49. Caers J, Verlinden H, Zels S, Vandersmissen HP, Vuerinckx K, Schoofs L. More than
713 two decades of research on insect neuropeptide GPCRs: an overview. Front
714 Endocrinol (Lausanne). 2012;3:151. doi: 10.3389/fendo.2012.00151.
715 50. Verbakel L, Lenaerts C, Vranken J, Marchal E, Broeck JV. Essential role of eclosion
716 hormone precursor and receptor genes in desert locust ecdysis. J Insect Physiol.
717 2024:104736. doi: 10.1016/j.jinsphys.2024.104736.
718 51. Ewer J, De Vente J, Truman JW. Neuropeptide induction of cyclic GMP increases in
719 the insect CNS: resolution at the level of single identifiable neurons. J Neurosci.
720 1994;14:7704-12.
721 52. Ewer J, Truman JW. Increases in cyclic 3',5'-guanosine monophosphate (cGMP)
722 occur at ecdysis in an evolutionarily conserved crustacean cardioactive peptide-
723 immunoreactive insect neuronal network. J Comp Neurol. 1996;370:330-41.
724 53. Lahr E, Dean D, Ewer J. Genetic analysis of ecdysis behavior in *Drosophila* reveals
725 partially overlapping functions of two unrelated neuropeptides. J Neurosci.
726 2012;32(20):6819-29. doi: 10.1523/JNEUROSCI.5301-11.2012.
727 54. Alon U. An Introduction to Systems Biology. 2nd Edition ed2019.

728 55. Davidson EH. Emerging properties of animal gene regulatory networks. Nature.
729 2010;468(7326):911-20. doi: 10.1038/nature09645.
730 56. Silva V, Palacios-Muñoz A, Volonté M, Frenkel L, Ewer J, Ons S. Orcokinin
731 neuropeptides regulate reproduction in the fruit fly, *Drosophila melanogaster*. Insect
732 Biochem Mol Biol. 2021;139:103676. doi: 10.1016/j.ibmb.2021.103676.
733 57. Lee D, Orchard I, Lange AB. Evidence for a conserved CCAP-signaling pathway
734 controlling ecdysis in a hemimetabolous insect, *Rhodnius prolixus*. Frontiers in
735 neuroscience. 2013;7:207.. doi: 10.3389/fnins.2013.00207.
736 58. Wulff JP, Sierra I, Sterkel M, Holtof M, Van Wielendaele P, Francini F, et al. Orcokinin
737 neuropeptides regulate ecdysis in the hemimetabolous insect *Rhodnius prolixus*.
738 Insect Biochem Mol Biol. 2017;81:91-102. doi: 10.1016/j.ibmb.2017.01.003.
739 59. Sullivan LF, Barker MS, Felix PC, Vuong RQ, White BH. Neuromodulation and the
740 toolkit for behavioural evolution: can ecdysis shed light on an old problem? FEBS J.
741 2022. doi: 10.1111/febs.16650.
742 60. Schindelin J, Arganda-Carreras I, Frise E, Kaynig V, Longair M, Pietzsch T, et al. Fiji:
743 an open-source platform for biological-image analysis. Nat Methods. 2012;9(7):676-
744 82. doi: 10.1038/nmeth.2019.
745 61. Hamada FN, Rosenzweig M, Kang K, Pulver SR, Ghezzi A, Jegla TJ, et al. An internal
746 thermal sensor controlling temperature preference in *Drosophila*. Nature.
747 2008;454(7201):217-20. doi: 10.1038/nature07001.
748 62. Nakai J, Ohkura M, Imoto K. A high signal-to-noise Ca(2+) probe composed of a
749 single green fluorescent protein. Nat Biotechnol. 2001;19(2):137-41. doi:
750 10.1038/84397.

751 63. Miller JE, Ayzenshtat I, Carrillo-Reid L, Yuste R. Visual stimuli recruit intrinsically
752 generated cortical ensembles. Proc Natl Acad Sci U S A. 2014;111(38):E4053-61. doi:
753 10.1073/pnas.1406077111.
754 64. Patel TP, Man K, Firestein BL, Meaney DF. Automated quantification of neuronal
755 networks and single-cell calcium dynamics using calcium imaging. Journal of
756 neuroscience methods. 2015;243:26-38. doi: 10.1016/j.jneumeth.2015.01.020.

757 **FIGURES**

758

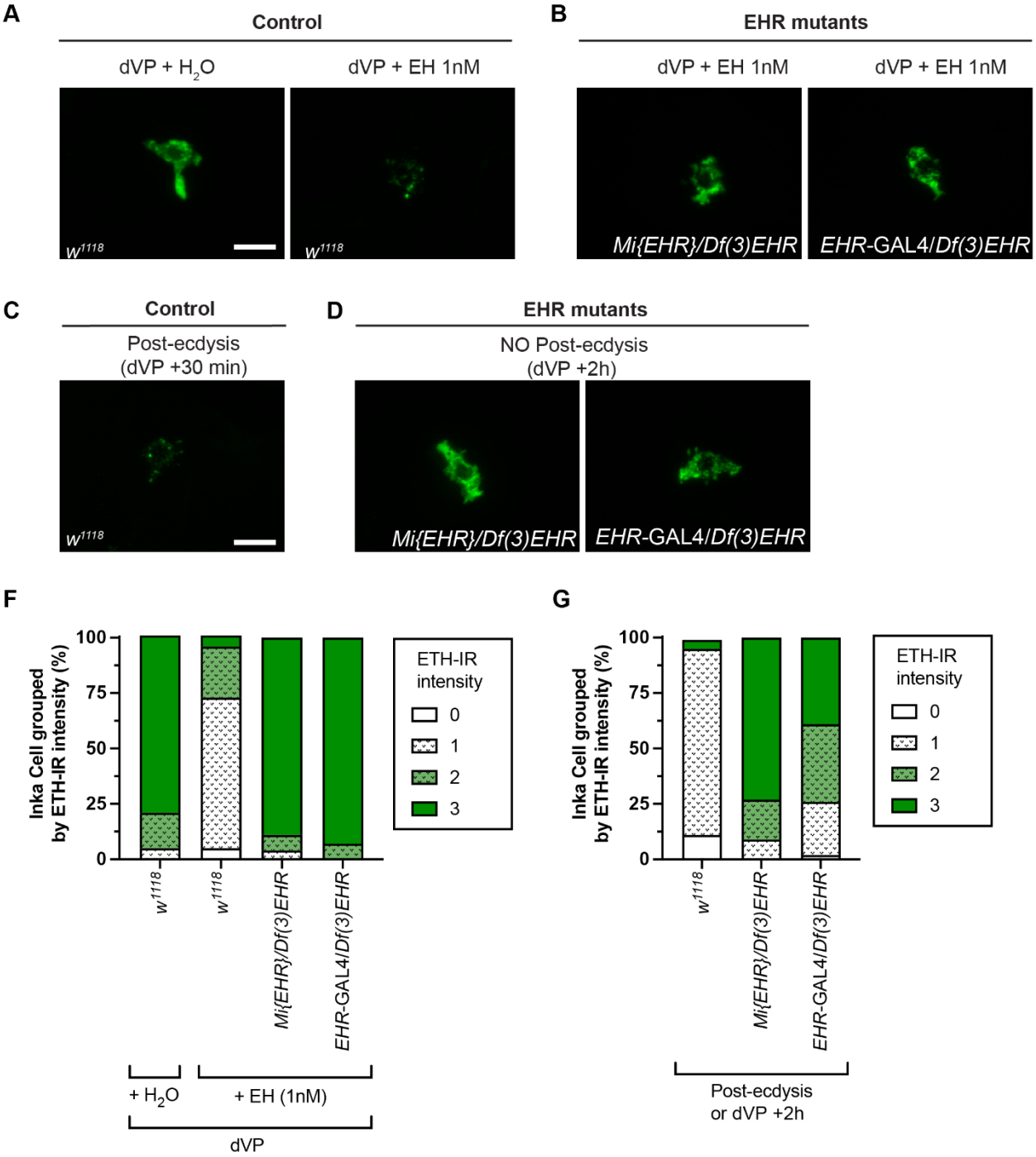

759

760 **Figure 1: Genetic lesions in CG10738 abolish EH-induced ETH release.**

761 (A) Immunoreactivity to ETH (ETH-IR) of epitracheal Inka cells from control animals

762 (w^{1118}) before (left) and after (right) *in vitro* stimulation with synthetic EH. (B) ETH-IR of

763 epitracheal cells of EHR mutant animals, *Mi*{*EHR*}/*Df(3)EHR* (left) and *EHR*-
764 GAL4/*Df(3)EHR* (right), after *in vitro* stimulation with synthetic EH. (C) ETH-IR of
765 epitracheal cells of wildtype (w^{1118}) animals after ecdysis. (D) ETH-IR of epitracheal cells
766 of EHR mutant animals, *Mi*{*EHR*}/*Df(3)EHR* (left) and *EHR*-GAL4/*Df(3)EHR* (right), 2h
767 after dVP stage. (F, G) Quantification of ETH-IR intensity for experiments depicted in
768 (A) and (B), and (C) and (D), respectively (N: 30-60 ETH cells, corresponding to 3-7 larvae
769 per group). Data were analyzed by Chi-square test (see Supplementary Table S3). Scale
770 bar 10µm.
771

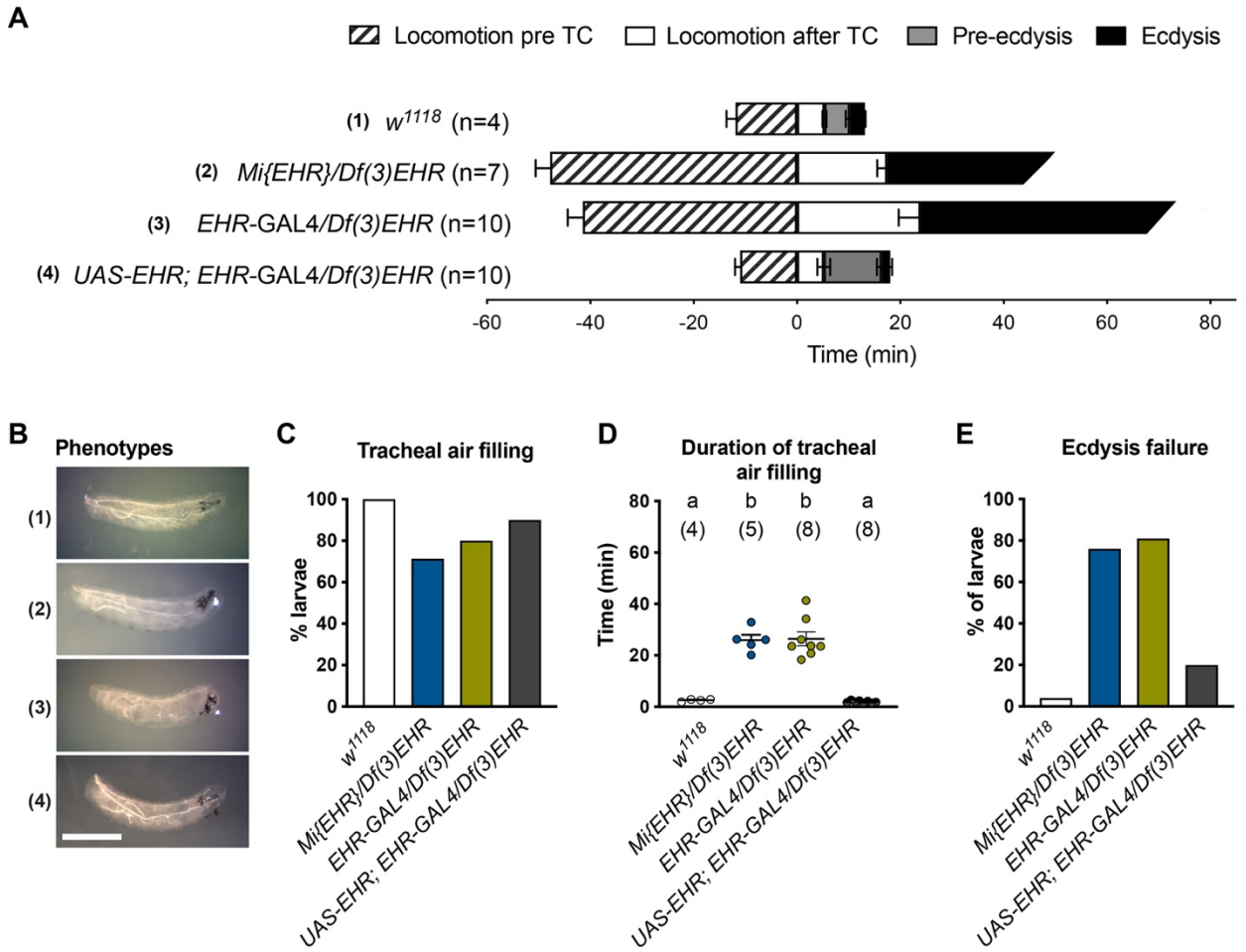

Figure 2: EHR mutant animals fail at the first larval ecdysis.

(A) Duration of the different phases of L1 to L2 larval ecdysis. Timeline has been aligned with respect to the time of tracheal collapse (TC). (B) Representative images of animals after ecdysis (for controls) or their terminal phenotype (for EHR mutants) for (1) Control (w^{1118}), (2) *Mi{EHR}/Df(3)EHR*, (3) *EHR*-GAL4/*Df(3)EHR*, and (4) UAS-*EHR; EHR*-GAL4/*Df(3)EHR* (genetic rescue) animals. (C) Percentage of animals that completely filled their trachea with air. (D) Duration of tracheal air filling (for animals that completed this process; N in parentheses). (E) Percentage of animals that failed larval ecdysis (N: 4-10 larvae per condition). Data were analyzed by unpaired *t*-test (A) one-way ANOVA and Tukey multiple comparison (D). Statistically significant differences are indicated by different letters in D (see Supplementary Table S3). Scale bar in (B) 500μm.

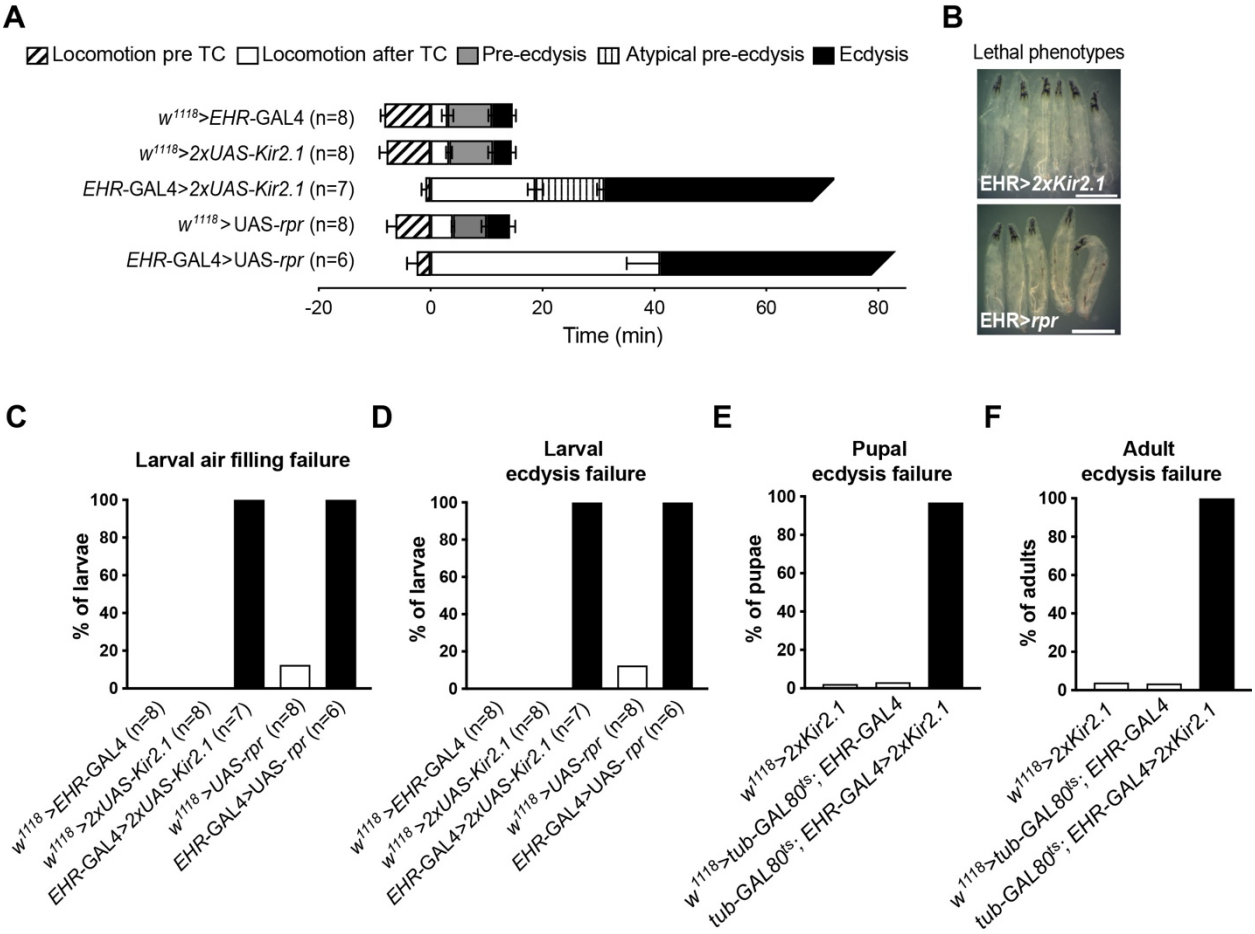

Figure 3: Ablating or inactivating EHR-expressing cells causes failures at larval, pupal, and adult ecdysis. (A) Duration of the different phases of L1 to L2 larval ecdysis; timeline has been aligned with respect to the time of tracheal collapse (TC). (B) Representative images of post-ecdysis or terminal phenotype of *EHR*>2x*Kir2.1* and *EHR>rpr* animals; (C) Percentage of animals that failed to fill their trachea with air; (D-F) percentage of animals that failed larval (D), pupal (E), and adult (F), ecdysis. (N: 150-500 per group for E-F). Data were analyzed by unpaired *t*-test (A) (see Supplementary Table S3). Scale bar 500μm

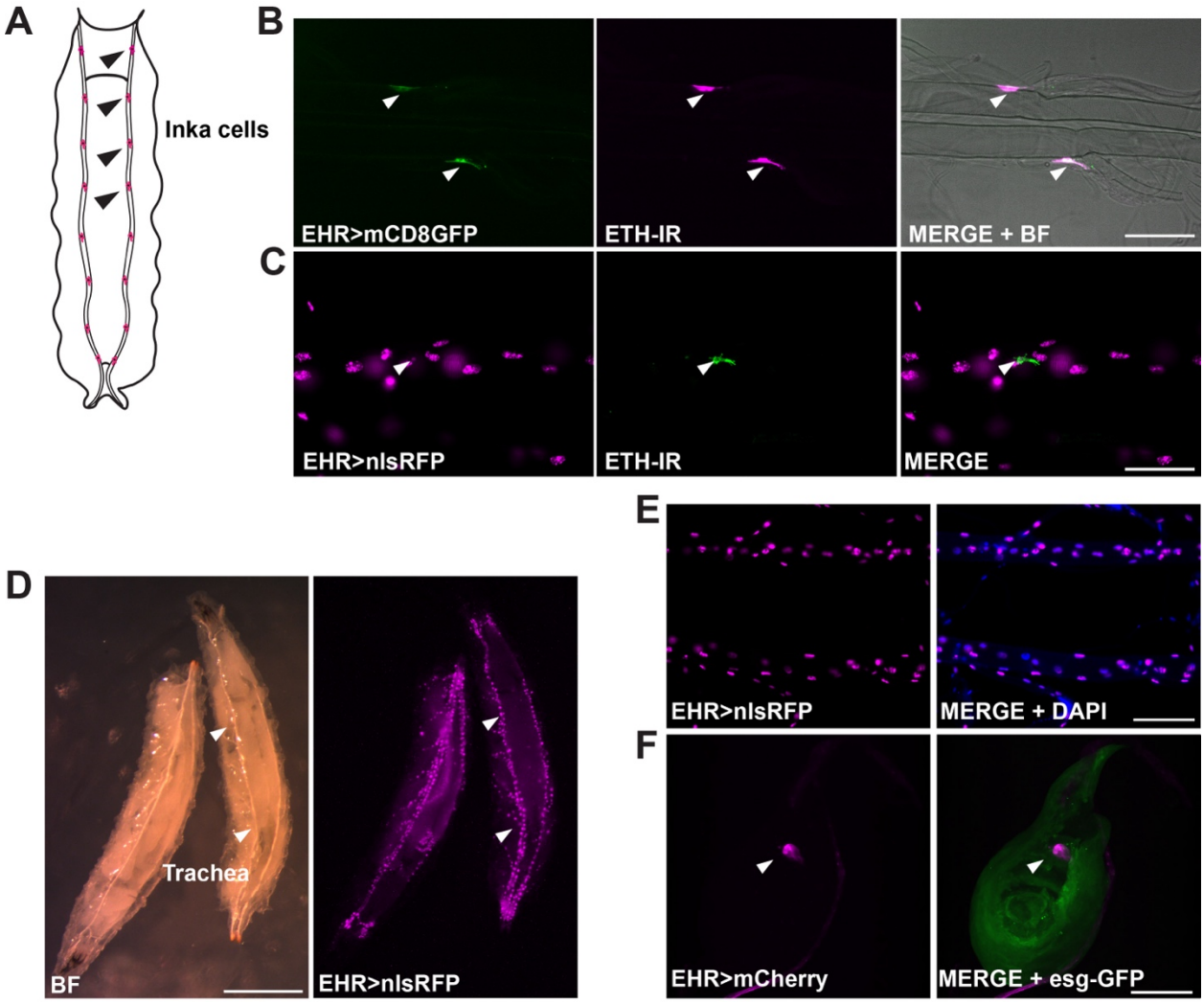

Figure 4: EHR is expressed in the ETH Inka cells, tracheal epithelial cells, and the leg imaginal disc of the third instar larva.

(A) Schematic representation of a larva showing the Inka cells (colored in magenta; four are indicated by black arrowheads), which are located along the dorsal trunks of the trachea. (B, C) EHR expression in Inka cell (white arrowhead) visualized using the membrane-bound form of GFP (B; *EHR*>mcd8GFP) or a nuclear version of RFP (C; *EHR*>nlsRFP), together with ETH-immunoreactivity. (In B, EHR expression in tracheal cells cannot be visualized unless gain is greatly increased, probably because the cells are too large to be strongly labeled with the membrane-bound GFP used; by contrast, they are readily visible using the nuclear reporter used in (C)). (D-E) EHR expression in tracheal epithelial cells visualized using a nuclear localized RFP transgene and counterstained with DAPI (E). (F) EHR expression in leg imaginal disc, labeled using the

809 *escargot* (*esg*)-GFP fusion protein. BF: bright field. Scale bars (B-C,E-F) 100μm, (D)
810 5mm.
811

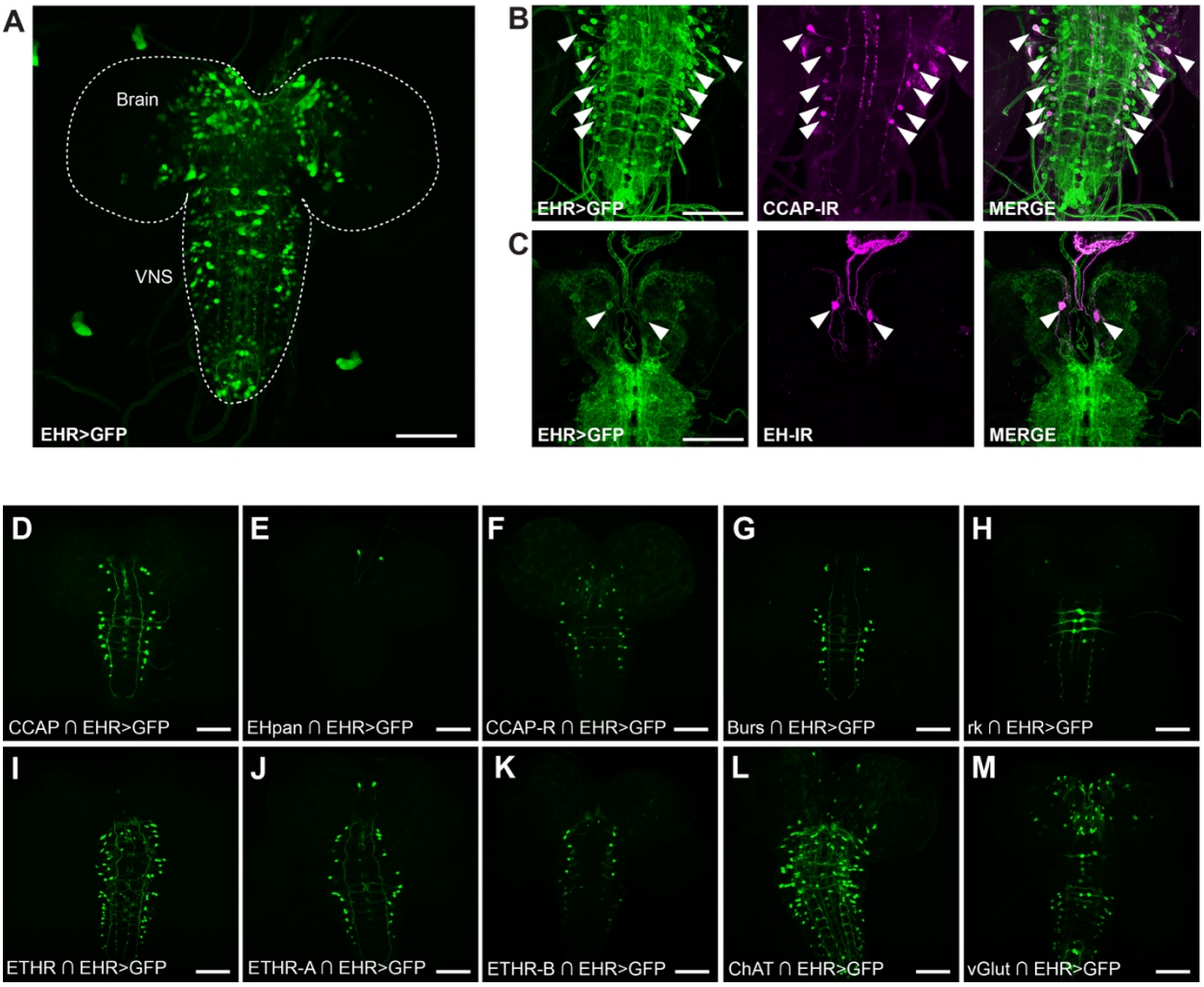

Figure 5: EHR expression in the larval CNS.

EHR is expressed in a large number of neurons in the 3rd larval instar CNS (A). In particular, EHR is expressed in CCAP neurons (B, D) and in Vm (EH) neurons (C, E). It is also expressed in neurons that express the CCAP receptor (CCAP-R) (F); in bursicon (G) and bursicon receptor (*rickets*) neurons (H); in neurons expressing the ETH receptor (ETHR) (I)(both its A (J) and B (K) isoforms); and in cholinergic (ChAT expression; L) and glutamatergic (vGlut expression; M) neurons. In (A) EHR expression was visualized using *EHR*>GFP; in (B, C), colocalization was established by co-immunolabeling with anti-CCAP (B) and anti-EH (C) antibodies; in (D-M) different subgroups of EHR-expressing neurons were visualized using appropriate "split"-GAL4 hemidrivers (indicated by intersection symbol, "∩") together with UAS-GFP. Scale bar 100μm.

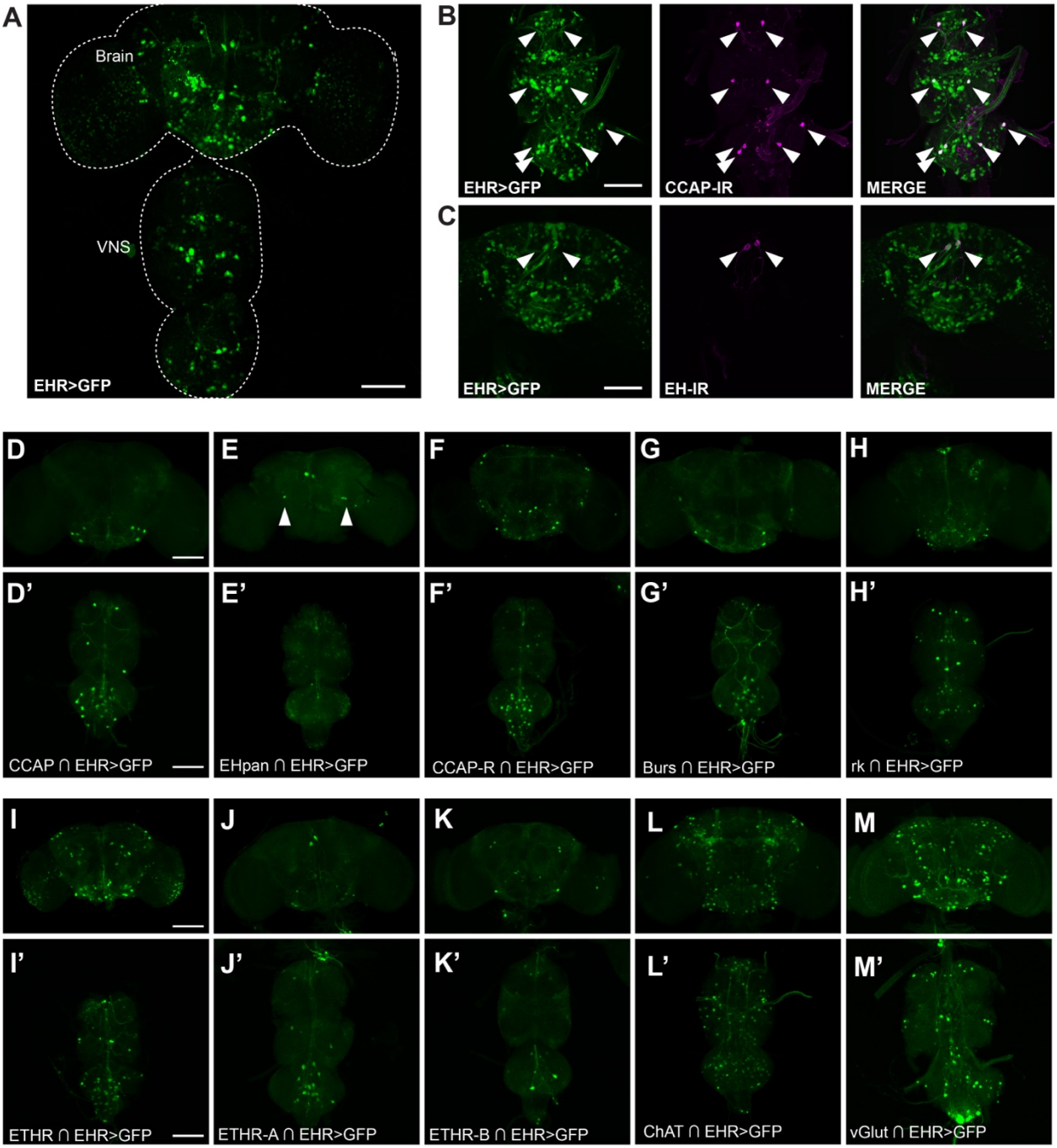

Figure 6: EHR expression in the pharate adult *Drosophila* CNS.

EHR is expressed in a large number of neurons in the pharate adult CNS (A). In particular, EHR is expressed in CCAP neurons (B, D) and in EH neurons (Vm: C, E and Dl: E, arrowhead). It is also expressed in neurons that express the CCAP receptor (CCAP-R) (F); in bursicon (G) and bursicon receptor (*rickets*) neurons (H); in neurons expressing

831 the ETH receptor (ETHR) (I)(both its A (J) and B (K) isoforms); and in cholinergic (ChAT
832 expression; L) and glutamatergic (vGlut expression; M) neurons. In (A) EHR expression
833 was visualized using *EHR*>GFP; in (B, C), colocalization was established by co-
834 immunolabeling with anti-CCAP (B) and anti-EH (C) antibodies; in (D-M) different
835 subgroups of EHR-expressing neurons were visualized using appropriate "split"-GAL4
836 hemidrivers (indicated by intersection symbol, "∩") together with UAS-GFP. Scale bar
837 100μm.
838

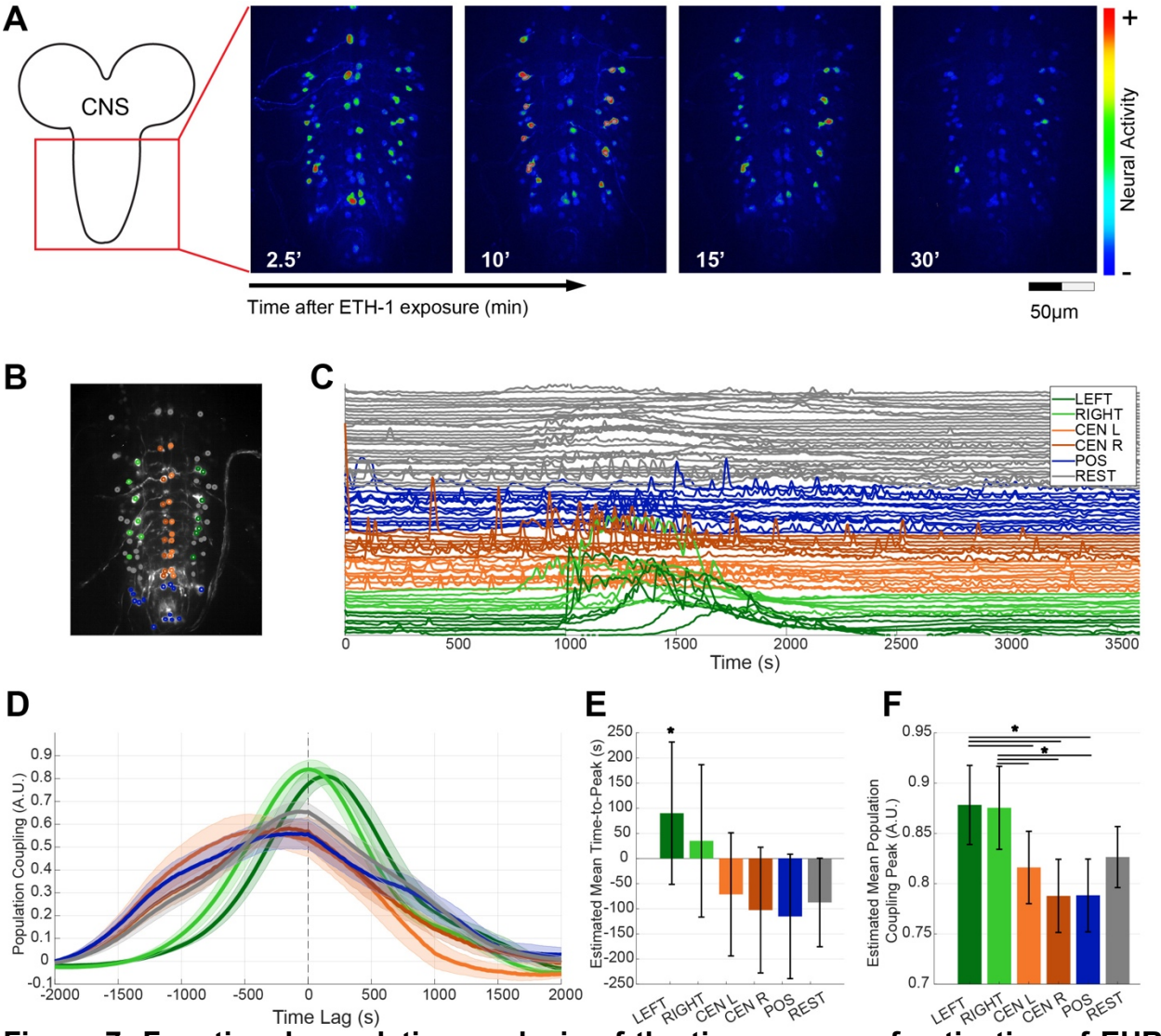

Figure 7: Functional population analysis of the time course of activation of EHR neurons in response to ETH stimulation *in vitro*.

(A) *Left:* Reference image of a pharate pupal CNS showing the area where the CNS response was recorded. *Right*: representative frames of GCaMP signal recorded *in vitro* from CNS expressing EHR>GCaPM6s, captured at different times after ETH challenge. CNSs were imaged for 1h, with images captured at a frequency of 0.2Hz. (B-F) Functional population analysis. (B) CNS with different subpopulations of EHR neurons color coded based on their position: "Left" (dark green) and "Right" (light green), which are likely made up mostly of CCAP neurons; "Central Left" neurons (orange); "Central Right" neurons (dark orange); "Posterior" neurons ("POS", blue); and the remaining ("REST") neurons (gray). (C) Timeseries of GCaMP6s signal following the same color

850 code used in B. Note the increased calcium activity around ~1000 s (15 min) after
851 stimulation with ETH (see also Supplementary Video 1). (D) Population coupling function
852 for the 6 different cell types for the CNS shown in (B) and (C). Solid lines represents the
853 average for all the cells of the same type and shaded area is the standard error. Positive
854 lag values means that the population activates after a given cell. (E) Estimated mean
855 time to peak of the functional population coupling function (PCF) from 5 different
856 experiments. Asterisk denotes statistically significant differences (* $p<0.05$) estimated
857 using a linear-mixed effect model. (F) Estimated mean peak of the PCF. Horizontal lines
858 denote significant differences using Bonferroni test corrected Wilcoxon rank sum (*
859 $p<0.05$) (see details in Table S3). Estimations of means and confidence intervals were
860 derived using a linear-mixed effect model with experiments as random effects. Error bars
861 for (E) and (F) are 95% confidence intervals.
862

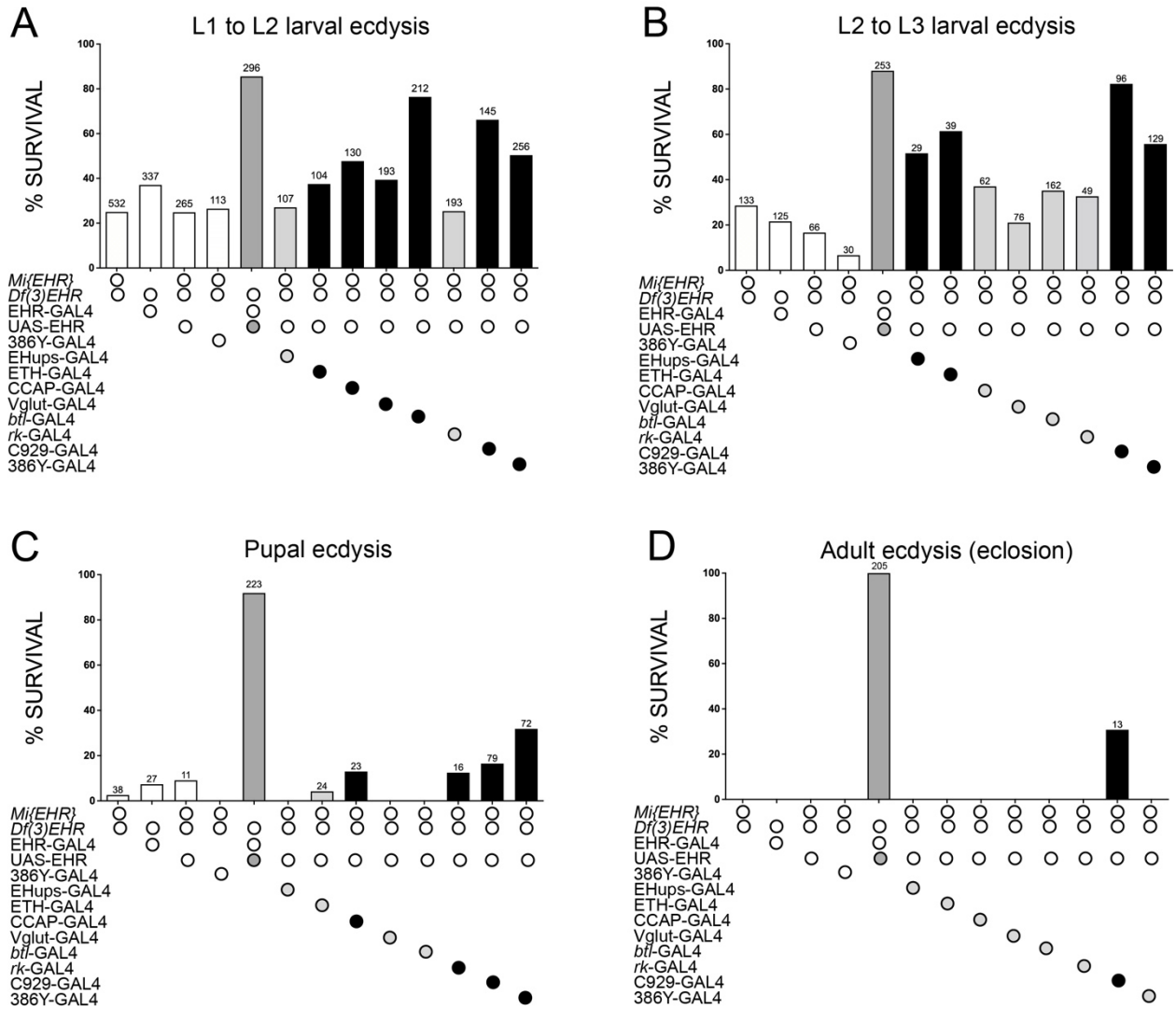

Figure 8: Rescue of ecdysial defects obtained by expressing EHR in subsets of EH targets.

Percentage of successful ecdysis from the first to the second (A) and second to the third (B) larval ecdysis, and for pupal (C) and adult (D) ecdysis, when EHR was expressed under the control of the indicated GAL4 drivers in an EHR mutant background. Open bars summarize the phenotype of the different EHR mutants used; the dark grey bars indicate the percentage of rescue obtained expressing EHR under the control of the EHR-GAL4 driver; the light gray and black bars summarize, respectively, the results obtained for genotypes that did not (light gray bars) and did (black bars) produce substantial levels of rescue compared to animals of the corresponding mutant genetic background. Numbers

874 above bars indicate the number of animals examined for that ecdysis. Values and
875 percentages are shown in Table 2.
876
877

878 **Table 1: Percentage of ecdysial failure caused by downregulation of EHR in**
879 **specific subsets of cells.** Drivers causing frequent failures (20% or greater) are
880 highlighted in orange.
881

GAL4 Driver	L1 to L2	L2 to L3	Pupal	Adult
w[1118] (control)	0% (0/101)	0% (0/73)[1]	0% (0/72)	0% (0/93)
General				
tubulin	47% (73/156)	95% (79/83)	100% (4/4)	N/A[2]
tsh	0% (0/24)	0% (0/48)	4.5% (3/67)	0% (0/64)
Peptidergic cells				
c929	26% (7/27)	29% (23/80)	95% (53/56)	N/A
386Y	1.4% (1/73)	0% (0/108)	100% (122/122)	N/A
sNPF	*ok*[3]	*ok*	*ok*	0% (0/94)
CCAP	0% (0/25)	0% (0/48)	1.7% (2/121)	0% (0/53)[4]
burs	0% (0/85)	0% (0/112)	0.6% (1/175)	1.1% (2/174)
EHups	3.3% (1/30)	39% (19/49)	0% (0/27)	0% (0/27)
Ehpan	9.4% (6/64)	3% (2/67)	1% (1/94)	4.4% (4/91)
ETH	0% (0/118)	69% (59/85)	100% (87/87)	N/A
Neuronal classes				
n-syb	0% (0/19)	0% (0/37)	100% (146/146)	N/A
v-Glut	0%	10% (13/130)	0.9% (1/117)	5.2% (6/116)
ChAT	0% (0/41)	0% (0/56)	0% (0/112)	0.9% (1/112)
DDC	0% (0/26)	0% (0/54)	0% (0/46)	0% (0/51)
ple	0% (0/65)	0% (0/58)	0% (0/117)	0% (0/151)
trhn	0% (0/65)	0% (0/62)	0.6% (1/174)	0% (0/188)
GAD1	*ok*	*ok*	*ok*	0% (0/30)
c164	7.1% (2/28)	0% (0/38)	6.4% (5/78)	2.7% (2/73)
nompC	*ok*	*ok*	*ok*	0% (0/74)
Gr66a			*ok*	0% (0/146)
109(2)80			*ok*	0%
Ir20a			*ok*	0%
Ir8a			*ok*	0% (0/56)
Smid c161			*ok*	0% (0/77)
Ir25a	-	20% (32/159)	8.7% (11/127)	5.2% (6/116)
Ir7g	-	14% (42/306)	10% (26/253)	0.8% (2/239)
Ir40a	-	6.9% (10/144)	1.5% (2/134)	3% (4/132)
410-GAL4	-	15% (22/152)	3.8% (5/130)	4% (5/125)
Ecdysis peptide receptors				
ETHR	9.6% (27/280)	13% (32/253)	5% (11/221)	0.4% (1/210)

CCAP-R	*ok*	*ok*	*ok*	0% (0/23)
rk	*ok*	*ok*	*ok*	0% (0/46)
Other cells				
repo	4.8% (2/42)	0% (0/84)	0% (0/94)	7.1% (7/99)
btl	4% (2/50)	0% (0/52)	54% (44/82)	92% (35/38)

[1] Fraction (and associated percentage) indicates the number of animals that failed at that ecdysis (in this case, fraction of 2nd instars that failed at ecdysis to the 3rd instar).

[2] No animals were obtained at this stage because an earlier ecdysis was lethal.

[3] The genotype of these animals could not be determined until after adult emergence, but no defects were observed at the larval or pupal stages.

[4] 32/53 (60%) showed abnormal wing expansion.

889 **Table 2: Success of genetic rescue of EHR lethal phenotype by expressing EHR in**
890 **specific subsets of EHR-expressing cells.** Cells marked in green indicate that a
891 substantial rescue was observed (as compared to phenotype of the corresponding mutant
892 control); lighter green indicates possible rescue. These data are also summarized
893 graphically in Figure 8.

Genotype	L1 to L2	L2 to L3	Pupal	Eclosion
% Ecdysis Success in Mutant controls				
Mi{EHR}/Df(3)EHR	25% (133/532)	29% (38/133)[1]	2.6% (1/38)	(1/1)[2]
EHR-GAL4/Df(3)EHR	37% (125/337)	22% (27/125)	7.4% (2/27)	0% (0/2)
UAS-EHR; Mi{EHR}/Df(3)EHR	25% (66/265)	17% (11/66)	9% (1/11)	(1/1)[2]
386Y, Mi{EHR}/Df(3)EHR	27% (30/113)	6.6% (2/30)	0% (0/2)	N/A[3]
% Ecdysis Success with Rescue of EHR function				
UAS-EHR; EHR-GAL4/Df(3)EHR	86% (253/296)	88% (223/253)	92% (205/223)	100% (205/205)
CCAP>EHR; Mi{EHR}/Df(3)EHR	48% (62/130)	37% (23/62)	13% (3/23)	0% (0/3)
ETH>EHR; Mi{EHR}/Df(3)EHR	38% (39/104)	62% (24/39)	4.2% (1/24)	0% (0/1)
EHups>EHR; Mi{EHR}/Df(3)EHR	27% (29/107)	52% (15/29)	0% (0/15)	N/A
Vglut>EHR; Mi{EHR}/Df(3)EHR	39% (76/193)	21% (16/76)	0% (0/16)	N/A
UAS-EHR; 386Y, Mi{EHR}/Df(3)EHR	50% (129/256)	56% (72/129)	32% (23/72)	0% (0/23)
C929>EHR; Mi{EHR}/Df(3)EHR	66% (96/145)	82% (79/96)	17% (13/79)	31% (4/13)
rk>EHR; Mi{EHR}/Df(3)EHR	25% (49/193)	33% (16/49)	13% (2/16)	0% (0/2)
btl>EHR; Mi{EHR}/Df(3)EHR	76% (162/212)	35% (57/162)	0% (0/57)	N/A

894 [1] Fraction (and associated percentage) indicates the number of animals that ecdysed to the next stage (in
895 this case, fraction of 2nd instars that ecdysed to the 3rd instar).
896 [2] Due to the low sample number, this outcome is not indicated as “100%” rescue.
897 [3] Success at this ecdysis could not be evaluated because an earlier ecdysis was lethal.
898